Biophysical Chemistry 147 (2010) 146–152

Contents lists available at ScienceDirect

Biophysical Chemistry

journal homepage: http://www.elsevier.com/locate/biophyschem

Anti-aggregation properties of trehalose on heat-induced secondary structure and conformation changes of bovine serum albumin

Davide Barreca [a], Giuseppina Laganà [a], Silvana Ficarra [a], Ester Tellone [a], Ugo Leuzzi [a], Salvatore Magazù [b], Antonio Galtieri [a], Ersilia Bellocco [a,*,1]

[a] Department of Organic and Biological Chemistry, University of Messina, Salita Sperone 31, Villaggio S. Agata, 98166 Messina, Italy
[b] Department of Physics, University of Messina, Salita Sperone 31, Villaggio S. Agata, 98166 Messina, Italy

ARTICLE INFO

Article history:
Received 30 December 2009
Received in revised form 22 January 2010
Accepted 25 January 2010
Available online 1 February 2010

Keywords:
Trehalose
BSA
Circular dichroism and IR-spectroscopy
Aggregation
Light scattering
Fluorescence

ABSTRACT

During our experimental work, aggregation of bovine serum albumin was obtained incubating the protein solution at 60 °C to investigate temperature-induced secondary structure, conformation changes and anti-aggregative activity of trehalose. IR-measurements suggested that in the presence of 1.0 M of trehalose there is a little increase in short segment connecting α-helical and a clearly decrease in the loss of α-helix structure and in the formation of intermolecular and antiparellel β-sheet up to 78 and 55%, respectively. Useful information also arose following the temperature evolution of Amide I′ band profile in the range of temperature between 25 and 90 °C in absence or in presence of 1.0 M trehalose. Complementary information is obtained by electrophoresis, circular dichroism, fluorescence spectroscopy, titration of SH groups and light scattering measurements. Results encouraged biotechnology and pharmaceutical application of the disaccharide and provided evidence for its utilization in degenerative diseases evolving via aggregation process.

1. Introduction

Prevention of protein aggregation is one of the most important aim of biochemical and biophysical researches, due to its unchallenged importance and application in biotechnology, industrial and pharmaceutical application. In fact, protein aggregation is associated with a large amount of neurodegenerative diseases, such as the amyloidoses, prion diseases and cataracts [1–3]. The protein interaction with small ligands often takes place with an increase in protein thermostability due to the coupling of binding with unfolding equilibrium. Trehalose (α,α-trehalose) has gained a position of remark among other kosmotrope due to its unique characteristics. It is a disaccharide widely distributed in nature, attracting the researches attention because it confers to certain plant and animal cells the ability to survive dehydration. Because trehalose is formed by the binding of the two reducing groups, it has no capacity to reduce other compounds. It is a well-known bioprotectant system capable of protecting many organisms in extreme life conditions, so many promising applications have been proposed for example in preserving vaccines, vitamins and biological macromolecules [4–6]. The aggregation process usually involves conformational changes of the whole protein or of a specific domain and it is often attributed to the association of partially unfolded molecules [7,8]. However, it is not yet fully understood how the conformational changes, at secondary and tertiary structure level, take part in the aggregation pathways. It is a common idea that the aggregation could occur via structural changes leading to formation of β richer structures. This observation is due to the fact that the core structure of all amyloid consists of β-sheets and short peptides, rich in hydrophobic residues and β-sheet, have the tendency to form aggregates [9]. The aggregation process is strongly affected by temperature, time of heating, concentration and pH too. Interesting studies have been carried out analyzing heat and pH denaturation of BSA [10–12].

Bovine Serum albumin (BSA) is one of the most studied proteins utilized as a model for many and diverse biophysical, biochemical and physicochemical studies [13]. It is the most abundant protein in blood plasma, accounting for about 60% of the total protein and 80% to colloid osmotic blood pressure. These proteins have the interesting properties in the binding of a variety of hydrophobic ligands (fatty acids, lysolecithin, bilirubin, warfarin, tryptophan, steroids, anaesthetics and several dyes), in the transport and deposition of a variety of endogenous and exogenous substances in blood due to the existence of a limited number of binding regions with different specificity [14]. Bovine serum albumin (BSA), with molecular mass 66,500 Da, is composed of 583 amino acid residues [15]. The secondary structure of BSA consists of approximately of 67% α-helix, 10% turn, and 23% extended chains, and no β-sheet is contained [13,15,16], originating nine loops and 17

* Corresponding author. Tel.: +39 090 6765184; fax: +39 090 393895.
E-mail address: bellocco@isengard.unime.it (E. Bellocco).
[1] Postal address: Department of Organic and Biological Chemistry — University of Messina. Salita Sperone, 31 (S. Agata) — 98166 Messina.

0301-4622/$ – see front matter © 2010 Elsevier B.V. All rights reserved.
doi:10.1016/j.bpc.2010.01.010

disulphide bridges. It consists of three homologous domains (I, II and III) which are divided into two sub-domains (A and B) [13–16]. In this paper, we report an experimental study aimed to single out information about anti-aggregative influences of trehalose on a model study protein (BSA). To this purpose, we perform kinetic data on thermal aggregation of BSA in presence or absence of trehalose, at different temperatures utilizing data obtained by electrophoresis, light scattering measurements, infrared (IR) and fluorescence spectroscopy.

2. Materials and methods

2.1. Infrared spectroscopy

Lyophilized BSA was purchased from Sigma Chemical Co. (St. Louis, MO). Prior to infrared experiments, the protein was dissolved in D_2O at 25 °C for 1 day and lyophilized from D_2O. This procedure was performed twice for each sample. The single-beam IR spectra, between 1350 and 1750 cm^{-1}, were measured with a Bruker Vertex 80 spectrometer. Before IR measurements, the sample were dissolved in Tris–HCl buffer pH 7.2 10 mM prepared in D_2O. The pD value of the BSA solution was measured with a standard pH electrode, and corrected according to pD = pH + 0.4 for deuterium isotope effects. The protein solution (60 ml/ml), in absence or presence of 1.0 M trehalose, was heated for 2 h in a water bath at 60 °C, placed between a pair of CaF_2 windows separated with a 25 μm Teflon spacer, and then was inserted in the fluid cell. For each measurement, were collected 128 interferograms with a spectral resolution of 2 cm^{-1}. IR spectra of a Tris–HCl buffer pH 7.2 10 mM with or without 1.0 M trehalose solution were measured under identical conditions and subtracted from the spectra of the protein at the corresponding temperature. Each measure was performed under vacuum to eliminated minor spectral contributions due to residual water vapor. The final protein spectra were used for further analysis.

2.2. Temperature dependent conformational changes

To obtain spectra at discrete temperatures, the protein solution (60 ml/ml), in absence or presence of 1.0 M trehalose, was heated with an interval of 5 °C between 25 and 90 °C. A spectrum at each temperature was obtained by equilibrating the sample for 5 min prior to data collection, and analyzed as above described by infrared spectroscopy.

2.3. Data analysis of IR spectra

Protein spectra were smoothed by Loess algorithm and the deconvolved spectra fitted with Gaussian band profiles. Initial values for the peak heights and widths were estimated from the deconvolved spectra. For the final fits, the positions, heights, and widths of all bands were varied simultaneously. The curve fitting procedure was calculated on Seasolve PeakFit v4.12 software.

2.4. Conformational changes monitoring by PAGE

BSA samples (1 μg/μl), incubated for 2 h at 60 °C in presence or absence of trehalose (0.25-1.0 M), were separated on a 10% PolyAcrylamide Gel Electrophoresis (PAGE). Samples were electrophoresed towards the anode at a constant voltage of 100 V for 2 h on a (mini)vertical electrophoresis unit purchased from BioRad, Hercules, CA, USA. The gels were stained with Coomassie blue R 250. Protein without incubation at 60 °C was utilized as reference status.

2.5. Gel image processing

Stained gels, digitized by image scanner, were processed by ImageJ software (available at the Web site http://rsb.info.nih.gov/ij/) which included background subtraction, contrast enhancement, dye front baseline correction and signal to noise enhancement.

2.6. Fluorescence measurements

Intrinsic and 1-anilino-naphtalene-8-sulfonate (ANS) fluorescence measurements of BSA (2.5 mg/ml) in Tris–HCl buffer pH 7.2 10 mM were carried out in the absence or in the presence of 0.25, 0.5 and 1.0 M trehalose using a spectrofluorometer. Intrinsic fluorescence spectra of the enzyme in absence or presence of the cosolvent were recorded after incubation at 60 °C for 2 h. The protein samples were excited at 280 and 295 nm to characterize a possible different behavior of tryptophan and/or tyrosine residues. It was observed that both spectra were similar. The rest of the experiment was acquired by excitation at 280 nm and emission spectra were recorded in the range of 320–400 nm. For measurements of the ANS fluorescence, BSA samples prepared as above described, were added of 200 μM of ANS after incubation at 60 °C for 2 h and analyzed by fluorescence. Appropriate checks of the respective cosolvent and ANS were taken to eliminate the interference in fluorescence spectra of the enzyme. The excitation wavelength was set at 380 nm and emission spectra were recorded in the range of 400–600 nm.

2.7. Light scattering measurements

Binary BSA/water and ternary BSA/trehalose/water solutions were prepared weighting and diluting fixed amount of solute in pure distilled water. BSA/water system has been studied in a limited concentration range of 0.0012–0.011 by weight dilute regime at the temperature values of 20–70 °C. As far as ternary systems are concerned, the BSA/water molar ratio was kept constant at 6.3×10^{-6}, chosen in order that the BSA concentration in water was in the dilute regime, but concentrated enough to have a good signal and reproducible correlation functions, whereas the trehalose amount was changed in order to obtain the same number of water molecules per each trehalose molecule. All the systems were carefully subordinate to a filtering procedure in recirculation with an Amicon Millipore filter 0.2 μm of diameter pore size, to obtain autocorrelation functions with a good signal-to-noise ratio. Quasielastic Light Scattering measurements were performed by means of a PCS technique, using a standard scattering apparatus with a photon counting optical system and a Brookhaven BI-2030 correlator to analyze the scattered light.

As exciting source, the 4880 Å vertically polarized line of a unimode Ar^+ laser Innova model 70, working in the power range of 50–700 mW, was used. The scattered light, by means of an optical fiber, was detected essentially in a 90° scattering geometry by a photomultiplier tube connected with the correlator. Samples were mounted in a thermostat with a temperature control better than ±0.02 °C. Viscosity measurements, useful for the characterization and interpretation of the ternary systems, were performed by means of standard Ubbhelode viscometers of different capillary size in order to minimize the kinetical energy corrections.

2.8. Data analyses

PCS allows us to measure the normalized autocorrelation function of the total scattered intensity $Is(q,t)$ [17]:

$$g_2(q,t) = \frac{\langle I_S(q,0) I_S(q,t) \rangle}{\langle I_S(q) \rangle^2}. \quad (1)$$

In the case of particle *motion independence*, the central limit theorem ensures that the scattered field will obey a Gaussian distribution, and the Siegert's relationship can be applied:

$$g_2(q,t) = 1 + \alpha |g_1(q,t)|^2, \quad (2)$$

where a is a constant that depends on the number of the selected coherence areas and hence on the experimental setup! $g1(q,t)$ is the normalized field autocorrelation function, defined as:

$$g_1(q,t) = \frac{\langle E_S(q,0)E_S^*(q,t)\rangle}{\langle |E_S(q)|^2\rangle} = \frac{\langle E_S(q,0)E_S^*(q,t)\rangle}{\langle I_S(q)\rangle}. \quad (3)$$

In the time domain typical of a light scattering experiment ($\geq 10^{-6}$ s), that is for times between the characteristic viscous flow relaxation and the diffusive relaxation over a scale as great as particle dimension, hydrodynamic interactions can be considered as instantaneous and direct interactions do not affect the particle's configuration. Under these conditions and for monodisperse spherical scatterers, intensity correlation function decays exponentially, according to

$$g_1(q,t) = \exp[-\Gamma(q)t], \quad (4)$$

where $\Gamma(q)$ is the half-width at half-maximum of the optical spectrum, which, for $qR_H<1$, is related to the diffusion coefficient, D, by the relation $\Gamma = Dq^2$ [18]. From a general point of view, D is an *effective* q-dependent diffusion coefficient that depends on the particle equilibrium distributions ($S(q)$) as well as on the hydrodynamic interactions ($H(q)$)[19]:

$$D(q) = D_0\frac{H(q)}{S(q)}. \quad (5)$$

In the limit $q\rightarrow 0$, the effective diffusion coefficient is identified with the collective-diffusion coefficient, defined by the generalized Stokes–Einstein relation $D_c = (\partial\Pi\ /\partial c)_T[1\text{-}/\zeta(c)](1\text{-}Vc)$, with $(\partial/\partial\Pi)_T \propto [S(0)]^{-1}$ osmotic compressibility, ζ frictional coefficient, V molecule partial specific volume, and c the concentration. It should be noticed that since $S(q\rightarrow 0)$ can become very small compared to 1, the collective diffusion coefficient D_c can be much larger than the free diffusion coefficient at infinite dilution. Its concentration dependence gives information about intermolecular interactions. In the dilute regime, in fact, the first-order virial expansion can be applied:

$$D_c = D_0(1 + k_D c). \quad (6)$$

The sign and magnitude of the slope, k_D, is related, neglecting the contribution of the volume V to frictional and osmotic compressibility virial coefficients, and, hence, to direct and frictional interaction character, by [20]

$$k_D = 2A_2M - B_\zeta, \quad (7)$$

with B_ζ the second virial coefficient of frictional interactions. In the very diluted limit, the theory of Brownian motion relates the measured D to the self-diffusion coefficient D_0 , which is connected to the center of mass motion of the isolated coil and allows us to evaluate the hydrodynamic radius, R_H , of the particles by the Einstein–Stokes (ES) relation:

$$D_0 = \frac{K_B T}{6\pi\eta R_H}, \quad (8)$$

where η is the viscosity coefficient of the continuous medium. As a matter of fact, polymeric solutions, especially with polymers at a high molecular weight, are polydisperse, so $g_1(t)$ becomes nonexponential because of the presence of a relaxation time distribution originated by the distribution of particle sizes. Consequently, in such a case for the $g_1(t)$ the Kohlraush–Williams–Watt (KWW) function is more suitable:

$$g_1(t) = A\exp\left[-\left(\frac{t}{\tau_{KWW}}\right)^{\beta_{KWW}}\right], \quad (9)$$

where β_{KWW}, which ranges from 0 to 1, is the shape parameter measuring the broadening of the relaxation time distribution. The average diffusive relaxation time is related to τ_{KWW} by $\langle\tau\rangle = (\tau_{KWW}/\beta_{KWW})\Gamma(1/\beta_{KWW})$, with $\Gamma(x)$ the gamma function. For the analysis of protein/water systems this latter approach has been preferred to the more usual cumulant analysis in order to obtain more quantitative information from the analysis of the protein/trehalose/water system correlation functions, where a net distinction between two diffusive decays occurs.

2.9. Circular dichroism (CD) spectra measurements

Circular dichroism measurements were made with a Jasco J-810 automatic spectropolarimeter. The protein (8.3×10^{-7} M) were dissolved in 10 mM Tris–HCl buffer (pH 7.2) in absence or presence of 1.0 M trehalose and incubated for 2 h at 60 °C. As reference spectra were used the one of protein incubated for 2 h in the same experimental condition but at the temperature of 37 °C. The spectra were registered at room temperature by using accumulation and time integration to improve signal-to-noise ratio. Each spectrum was corrected for baseline by subtracting the spectral contribution of the buffer solution or buffer plus additive. The far-UV spectra of protein were recorded between 190 and 260 nm using a quartz cell of 1.0 cm.

2.10. Titration with 5,5′-dithio-bis-2-nitrobenzoic acid (DTNB)

A solution containing the required amount of protein was dissolved in Tris–acetate buffer 50 mM pH 8.0 with 1.0 mM EDTA. The protein, in a final volume of 0.5 ml, was preincubated at 25 and 60 °C with or without 1.0 M of trehalose and afterwards suitable amounts of the sulfydryl reagent DTNB were added. DTNB (80-fold molar excess with respect to protein) was prepared in the same buffer. The reaction starts after DTNB addition. The reaction was monitored by the change in absorbance at 412 nm. The number of sulfydryl groups titrated was calculated using the extinction coefficient (13,600 M^{-1} cm^{-1}) of 2-nitro-5-mercaptobenzoic acid (TNB), released after the reaction of DTNB with protein-SH-group [21]. The protein concentration was calculated assuming a molecular mass of 66,500 Da.

3. Results and discussion

To single out information about the aggregation pathway, we investigated the thermally induced conformational and structural changes of bovine serum albumin in absence or presence of trehalose.

Previous studies on heat-induced BSA denaturation [10–12] showed that the protein did not denature up to 40 °C and its conformational changes were reversible in the temperature range of 42–50 °C. Otherwise unfolding of α-helix of BSA was irreversible in the temperature range of 52–60 °C and from 60 °C aggregation of the molecule happened. Fig. 1 showed absorption spectra in the Amides region of a BSA sample at 37 °C and after 2 h of incubation at 60 °C in absence or presence of 1.0 M trehalose.

The IR spectrum of BSA at 37 °C before heating was dominated by bands due to the amide I′ (mainly C=O stretching vibration), amide II (coupling of the N–H bending and C–N stretching modes), amide II′ (coupling of the N–D bending and C–N stretching modes) modes and side chain vibrations [22–24]. As can be seen, BSA exhibited an intense Amide I′ band centered at approximately 1652 cm^{-1}, corresponding mainly to α-helix structure content. After incubation at 60 °C, the intensity of this band decreased, suggesting a partial loss of the α-helix structure. Moreover, this decreasing was accompanied by the appearance of two shoulders at 1615 and 1682 cm^{-1}, that were attributed to the formation of aggregates [25,26]. In particular, the band at 1682 cm^{-1} was assigned to the antiparallel β-sheet whereas the other band at 1615 cm^{-1} was due to the intermolecular β-sheets resulting from

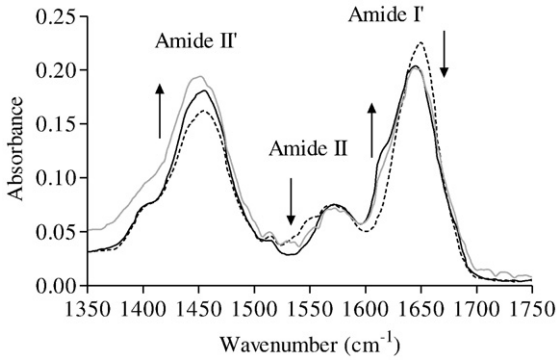

Fig. 1. IR absorption spectra of BSA at 37 °C (dotted line) and after 2 h of incubation at 60 °C in absence (solid dark line) or presence of 1.0 M trehalose (solid grey line). The arrows indicate the changes in the main Amide band profiles from native to aggregated protein state.

the aggregation. In the presence of 1.0 M trehalose after incubation at 60 °C, there was a decrease in the intensity around 1652 cm^{-1}, but the shoulder at 1615 cm^{-1} was much more less pronounced. Moreover, as clearly shown in Fig. 1, both Amide II and Amide II′ spectral contributions were present and, in particular, before and after 2 h at 60 °C, one decreased and the other one increased. This suggested that the hydrogen remained within the core of the protein can undergo to H–D exchange during the incubation time, as the protein partially unfolded. The decrease of Amide II at approximately 1540 cm^{-1} and the increase of Amide II′ at approximately 1450 cm^{-1} was strictly related, suggesting conformational changes at the tertiary structural levels. The bands observed between 1600 and 1500 cm^{-1} were attributed mainly to amino acid side chains contribution. In particularly the band was attributed to the aminoacid asparagine (near 1585 cm^{-1}), glutamine (near 1570 cm^{-1}) and arginine (near 1586 cm^{-1}), while the band at 1570 cm^{-1} and 1515 cm^{-1} to glutamate and tyrosine contribution [9,27,28]. The band at ~1515 cm^{-1} due to tyrosine (Tyr) provides a specific local monitor for conformational changes [22–27]. In fact the aromatic ring stretching vibration of the aminoacid residue was well distinguished in the spectra of protein. According to literature [22], an absorbance change in the Tyr band is observed when hydrophobic cores of a protein are formed, as solvent is excluded from the vicinity of Tyr residues that are buried in native protein molecule. Three of the six Tyr residues in BSA are buried in the native molecule whereas the other three are located on the protein surface [13]. Fig. 1 showed a clearly decrease in the peak intensity of the Tyr band after incubation at 60 °C for 2 h, while in presence of 1.0 M trehalose it is even increased. During heat-induced denaturation of a protein, Tyr band intensity and shift can be correlated with the strengthening of the OH group of Tyr and with the loosening of hydrogen bonds between the OH group of Tyr and neighboring acceptors. Thus, the results in Fig. 1 indicated that the conformation change of BSA after incubation at high temperature led to the loosening and/or destruction of specific hydrogen bonds of Tyr groups inside the protein, while the trehalose presence on the contrary contribute to preserve and enhanced the formation of this interaction. Other useful information arose analyzing the protein secondary structure of spectra reported in Fig. 1. The band assignments in the amide I′ band region can be made according to crystal structure of human serum albumin and previously published works [13–16,26]. The second derivative spectra of enzyme incubated at 37 °C revealed the presence of four bands centered at 1652, 1640, 1667 and 1630 cm^{-1} in the amide I′ region. The band at 1652 cm^{-1} was due to α-helical structures and around 1667 cm^{-1} was associated with turn structures [13–26]. The band at 1630 cm^{-1} was assigned to short-segment chains connecting α-helical segments of BSA. Traces of disordered structure were also evidenced at 1640 cm^{-1} (Table 1). At 60 °C, there was a clearly loss of α-helical and short segment connecting α-helical segments content and the appearance of two bands attributed to BSA

Table 1
Secondary structure content of BSA obtained by deconvolved spectra of Amide I′.

Structure	Amide I′ band/cm^{-1}	BSA 37 °C	BSA 60 °C	BSA 60 °C + trehalose 1.0 M
α-helix	1652	64 ± 3	45 ± 2	55 ± 3
Intermolecular β-sheet	1615	0	19 ± 3	4 ± 1
Antiparallel β-sheet	1682	0	9 ± 1	4 ± 1
Disordered structure	1640	1 ± 0.3	3 ± 1	1 ± 0.5
Turns	1667	9 ± 2	11 ± 2	5 ± 2
Short segment connecting α-helical segments	1630	26 ± 1	13 ± 2	31 ± 3

aggregation. In the presence of trehalose there was also a decrease, albeit inferior, in α-helical content, an increase in short segment connecting α-helical segments and a remarkable inhibition of intermolecular and antiparellel β-sheet up to 78 and 55%, respectively (Table 1). To explore the temperature-induced changes in secondary structure or aggregation of BSA in detail, we concentrated on the amide I′ region in the IR spectra, between 1600 and 1700 cm^{-1} that consists of overlapping component bands arising from different secondary structure elements. Fig. 2 reported the kinetic of IR spectra of BSA in presence or absence of 1.0 M trehalose, in the range of temperature between 25 and 90 °C. A comparison of the data showed a substantial difference in the evolution of the spectra. BSA spectra in the range of 25–55 °C didn't reveal any significant changes (Fig. 2a). In the range of temperature between 60 and 90 °C there was a clearly decreasing at 1652 cm^{-1}, accompanied by the appearance of the shoulders at 1615 and 1682 cm^{-1}. Furthermore, the observed isosbestic points suggested that the aggregation is a complex process that surely involves α-helix → aggregated β-sheet transition. The spectra above 70 °C showed a decrease in amide I′ band centered at 1645 cm^{-1} and an increase of two sharp bands at 1682 and 1615 cm^{-1}. In addition, the bands at 1682 and 1615 cm^{-1} had been associated with aggregated, intermolecular β-sheets[29,30].The BSA spectra in presence of 1.0 M trehalose were almost perfectly overlapping in the range of temperature between 25 and 65 °C. Above this least temperature, changes took place rapidly with a decrease in amide I′ band centered at 1652 cm^{-1} and an increase of two sharp bands at 1682 and 1615 cm^{-1} (Fig. 2b). Protein conformational changes were followed also by PAGE. The gel pattern evidenced the presence of an electrophoresis band with good anionic migration, corresponding to protein in the active forms (Fig. 3) and a little fraction without electrophoresis mobility corresponding to aggregate and/or denatured one. The gel pattern also showed as the band's intensity of native form decreased, following incubation at 60 °C for 2 h, while clearly increased the intensity of the band without electrophoresis mobility. Similar results were obtained incubating the protein in presence of 0.25 M trehalose, while in presence of 0.5 M the band's intensity of active forms clearly increased. The presence of 1.0 M of trehalose in the reaction mix avoided, almost completely, the effects of incubation at 60 °C for 2 h (Fig. 3). Valuable information about the changes in the local conformations of the protein, in absence or presence of trehalose, were obtained monitoring the changes in intrinsic and ANS fluorescence of the enzyme at high temperature. BSA belongs to the protein of class B and its fluorescence emission comes solely from tryptophan, even the protein contains more tyrosine than tryptophan residues. In fact in the BSA primary structure there are two tryptophan residues one located in the hydrophobic pocket of the subdomains IIA and the second one in subdomain IB placed in a hydrophobic pocket near the surface [31]. Tryptophan residues contribution to fluorescence is due to the efficient transfer of the excitation energy by Forster's resonance transfer process from tyrosyl to tryptophanyl residues which are placed close together in the native structure of the protein. Fig. 4a reported the BSA fluorescence intensity in absence or in presence of 0.25, 0.5 or 1.0 M trehalose. The intrinsic fluorescence emission maximum (λmax) of BSA was found to be 340 nm. After thermal treatment of the enzyme at 60 °C for 2 h, the intrinsic fluorescence intensity clearly increased, indicating an increase of

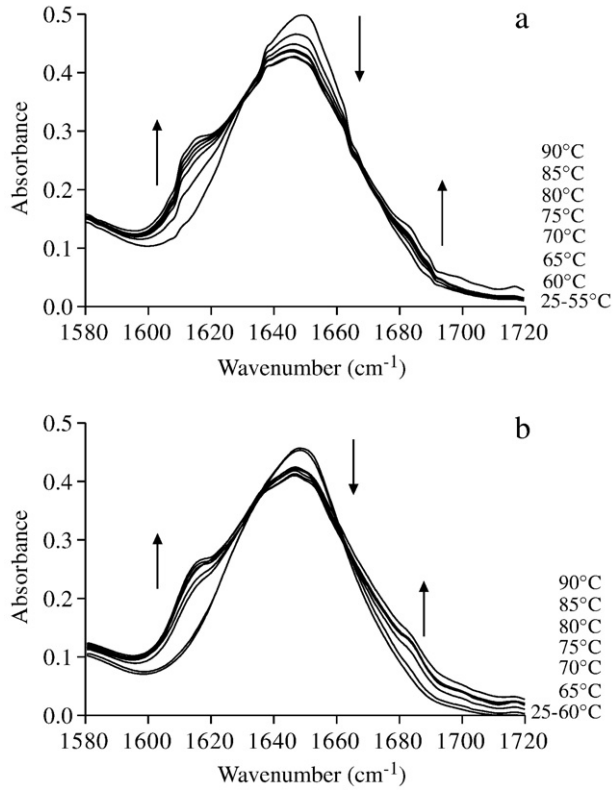

Fig. 2. Temperature evolution of amide I' spectral region of BSA, in the temperature range of 25–90 °C, in absence (a) or in presence of 1.0 M trehalose (b). The arrows indicate the changes in the main amide band profiles from native to aggregated form.

hydrophobicity of the environment around the mainly fluorescent groups. In the presence of 0.25, 0.5 and 1.0 M of cosolvent, the fluorescence intensity of the enzyme decreased. From the curves it is possible to observe that trehalose quenching of the intrinsic fluorescence of BSA was concentration dependent. Moreover, at all tested concentration, trehalose didn't induce changes in the maximum of emission peak, indicating a direct interaction with protein without modification of the hydrophobic environment. Further results arose from ANS binding experiments to BSA in absence or presence of trehalose. In fact it is a hydrophobic molecule, extensively used to probe the conformational changes that occur during protein denaturation, that binds preferentially to the hydrophobic clusters of the protein surface, and, in particular, with BSA subdomains IIA and IIIA [32]. After heat treatment, the ANS fluorescence intensity of BSA was found to be significantly increased. In the presence of the cosolvent, it was relatively lower than that of heat treated BSA (Fig. 4b). The structural changes induced by the temperature on BSA samples have been analyzed by light scattering measurements. Fig. 5 showed the time evolution of the total scattered intensity in absence or presence of trehalose. The hydrodynamic radius of BSA was major than that of the same molecules in presence of trehalose at all the analyzed temperatures, indicating that the disaccharide induced an increase in protein compactness. Moreover, as can be seen in the Fig. 5, the hydrodynamic radius of BSA increased markedly than the same macromolecule in presence of trehalose, reaching 1.3 fold at 70 °C. The results suggested the formation and growth of species precursor of aggregated protein that were markedly decreased in presence of the disaccharide. To further explore the structure conformation of BSA, far-UV circular dichroism analysis were carried out in presence or absence of 1.0 M trehalose in the range of 190–260 nm (Fig. 6). The CD spectrum of BSA, incubated at 37 °C for 2 h, showed the presence of two well defined negative bands at 208 and 222 nm, characteristic of macromolecules with high α-helical content [33]. The absorption in this region is due to peptide bond amide chromophore with a pronounced effect on the parallel polarized bands ($\pi \rightarrow \pi^*$ near 190 nm and $n \rightarrow \pi^*$ around 220 nm).The incubation of BSA at 60 °C for 2 h induced a marked decrease in both bands corresponding to an evident loss of protein α-helical. Also in the case of protein incubated at 60 °C in presence of the trehalose 1.0 M there was a decrease in the bands around 208 and 222 nm, although clearly inferior (Fig. 6). The CD spectra of BSA incubating at high temperature, in the presence or absence of trehalose, showed similar shape to the one of protein at 37 °C, indicating that the α-helical structure, albeit in minor quantities, were present. Moreover the decrease of the CD signal at around 210 nm was probably the result of enhanced flexibility of overall protein structure. BSA is a globular protein that contained 17 intrachain disulfide bonds and one free tiol group at residue 34 [13]. Cysteine (Cys) residues are often crucial to the function and structure of proteins and in the case of BSA the α-helical structure are mainly linked together by disulfide bridges, resulting in the formation of nine loops [34]. In our experiments, the

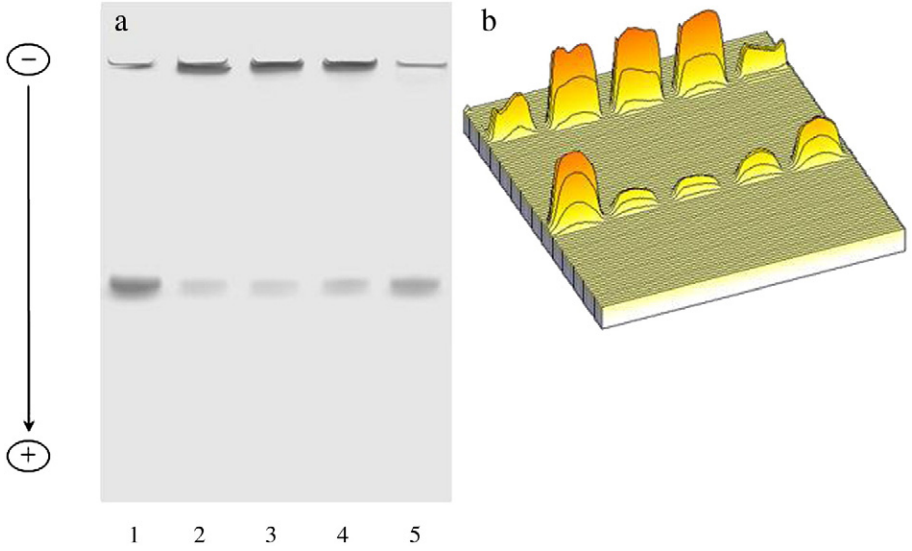

Fig. 3. PolyAcrylamide Gel Electrophoresis of BSA (1.0 mg/ml). a) Samples, pre-incubated at 60 °C in absence (2) or in presence of 0.25 M (3), 0.5 M (4), or 1.0 M (5) of trehalose, were electrophoresed toward the anode for 2 h. (1) Sample incubated in the same experimental condition at 37 °C without trehalose. b) Graphic elaboration of 3-D surface plot of electrophoresis pattern.

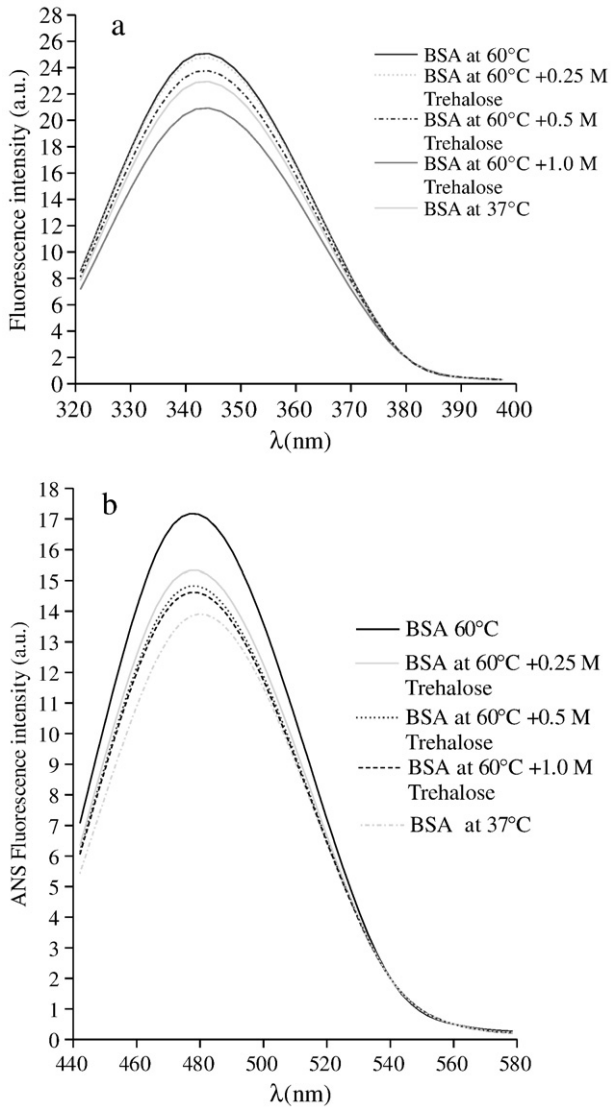

Fig. 4. Intrinsic (a) and ANS (b) fluorescence measurements of BSA (2.5 mg/ml) in the absence or in the presence of trehalose at different concentrations.

analysis of Cys residues has been performed utilizing DTNB. This molecule has been extensively used for probing free thiol groups and those arising from the eventually disruption of disulfide bonds in proteins, following the changes in absorbance at 412 nm. The reaction has been monitored either in presence or absence of 1.0 M trehalose. Stochiometry of BSA sulfhydryl groups reaction with DTNB revealed the

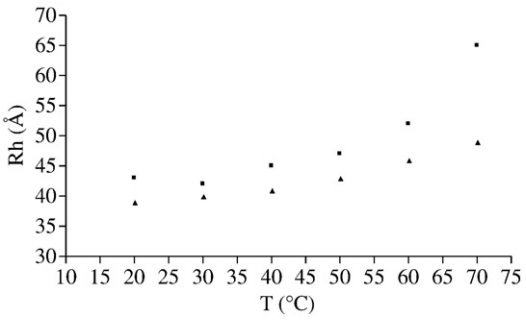

Fig. 5. The hydrodynamic radius versus temperature for BSA in absence (■) or presence (▲) of trehalose.

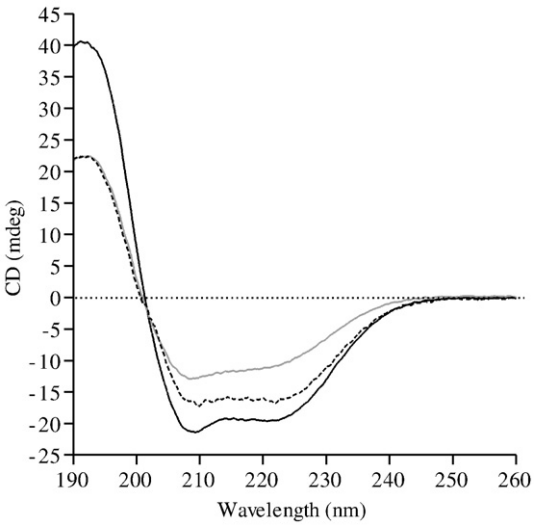

Fig. 6. Far-UV CD spectra of BSA. The spectra of protein (8.3×10^{-7} M), after incubation for 2 h at 37 °C (——) or at 60 °C in absence (——) or in the presence of 1.0 M trehalose (– – –), have been recorded between 190 and 260 nm.

presence of one free cysteine residue in the BSA sample after incubation at 37 °C for 2 h in absence or in the presence of 1.0 M trehalose. The same result have been obtained after incubation at 60 °C for 2 h of BSA samples both in absence and in the presence of 1.0 M trehalose.

4. Conclusion

Protein aggregation phenomena are involved in many different fields, from industry to medicinal and manufacture applications. It is often associated with conformational and structural changes that lead to exposure of peculiar protein residues, involving different mechanisms, whose time of occurrence and interplay can depend upon temperature and many other physical forces. In fact this complex process is not yet totally understood as it depends from a great number of physical and chemical parameters. The binding of small molecules to proteins and protein–protein interactions are key processes in cell biochemistry. It is well known that protein thermal stability is modified by ligand binding due to the coupling between two mutual processes under equilibrium: binding and unfolding. The additional binding free energy is responsible for shifting the unfolding temperature, and it could include or not contributions from conformational changes. Our experimental results clearly show the anti-aggregative properties of trehalose capable of reducing intermolecular and antiparellel β-sheet formation up to 78 and 55% using BSA as model protein. In solution, BSA, incubated alone, displays a temperature dependent increase in spontaneous aggregation. In fact after 2 h of incubation at 60 °C there is the formation of irreversible protein aggregated. Co-incubation with trehalose inhibits aggregation of this protein in a dose-dependent manner as shown by PAGE. High trehalose concentration (up to 1.0 M) avoids almost completely BSA aggregation. The key elements liable to aggregation of BSA after incubation at 60 °C, seem to be the decrease in α-helix and short segment connecting α-helical segments in favor of β-sheet. The trehalose presence in solution avoids the formation of β-sheet, although there is the decrease in α-helical structure, increasing markedly short segment connecting α-helix segments. These results also are supported by CD measurements. In fact, the incubation at high temperature, has a pronounced effect on protein structure. The α-helical structure content suffers a remarkable decrease, accompanied by a significant conformation change as revealed by the analyses of the macromolecule hydrodynamic radius, while in the presence of trehalose the entity of these variations is remarkably diminished. Moreover, the disaccharide preserves the microenvironment around

Tyr and enhances the formation of specific hydrogen bonds of the aminoacid with groups inside the protein. The trehalose influence is evident at level of the hydrophobic clusters of the protein surface too. In fact it decreases the accessibility of ANS to its preferentially binding site, in particular, with BSA subdomains IIA and IIIA, while in its absence they are markedly exposed at high temperature. Useful information also arises by intrinsic fluorescence measurements. In fact, while in absence of trehalose, there is a great increase in intrinsic fluorescence due to an enhancement in hydrophobicity following aggregation, trehalose presence dramatically decreases tryptophan fluorescence. Our results also underline that trehalose shift markedly the temperature for the aggregate formation from 60 to 70 °C. Light scattering evidences that the trehalose induces a major compactness of the protein structure as evidenced by hydrodynamic radius. These data are further supported by fluorescence measurements too. The titration of Cys residues with DTNB reveals that the total number of disulfide bonds remains unchanged and one free thiol group are recorded after incubation for 2 h at 60 °C, both in absence or presence of trehalose, as in the case of samples without incubation at high temperature. All the obtained results contribute to support the anti-aggregative properties of trehalose and its biotechnological application as a drug capable of interfering with production of aggregated structures, supporting evidence for its utilization in neurodegenerative pathologies such as Huntington's disease.

References

[1] V.N. Uversky, D.J. Segel, S. Doniach, A.L. Fink, Association induced folding of globular proteins, Proc. Natl. Acad. Sci. 95 (1998) 5480–5483.
[2] A.L. Fink, Protein aggregation: folding aggregates, inclusion bodies and amyloid, Fold. Des. 3 (1998) 9–23.
[3] R. Bauer, R. Carrotta, C. Rischel, L. Ogendal, Characterization and isolation of intermediates in α-lactoglobulin heat aggregation at high pH, Biophys. J. 79 (2000) 1030–1038.
[4] E. Bellocco, D. Barreca, G. Laganà, U. Leuzzi, F. Migliardo, G. Galli, A. Galtieri, L. Minutoli, F. Squadrito, Neutron scattering and HPLC study on L-ascorbic acid and its degradation, Chem. Phys. 345 (2008) 191–195.
[5] D. Barreca, E. Bellocco, G. Lagana`, U. Leuzzi, S. Magazu`, F. Migliardo, A. Galtieri, Spectroscopic investigation of structure-breakers and structure-makers on ornithine carbamoyltransferase, Food Chem. 106 (2008) 1438–1442.
[6] R.G. Strickley, B.D. Anderson, Solid-state stability of human insulin. II. Effect of water on reactive intermediate partitioning in lyophiles from pH 2–5 solutions: stabilization against covalent dimer formation, J. Pharm. Sci. 86 (1997) 645–653.
[7] A.H. Clark, D.H.P. Saunderson, A. Sugget, Infrared and laser-Raman spectroscopic studies of thermally induced globular protein gels, Int. J. Pept. Protein Res. 17 (1981) 353–364.
[8] P.L. San Biagio, V. Martorana, A. Emanuele, S.M. Vaiana, M. Manno, D. Bulone, M.B. Palma-Vittorelli, M.U. Palma, Interacting processes in protein coagulation, Protein Struct. Funct. Genet. 37 (1999) 116–120.
[9] J.S. Richardson, D.C. Richardson, Natural beta-sheet proteins use negative design to avoid edge-to-edge aggregation, Proc. Natl. Acad. Sci. U. S. A. 99 (2002) 2754–2759.
[10] K. Takeda, A. Wada, K. Yamamoto, Y. Moriyama, K. Aoki, Conformational change of bovine serum albumin by heat treatment, J. Protein Chem. 8 (1989) 653–659.
[11] V. Militello, V. Vetri, M. Leone, Conformational changes involved in thermal aggregation processes of bovine serum albumin, Biophys. Chem. 105 (2003) 133–141.
[12] V. Militello, C. Casarino, A. Emanuele, A. Giostra, F. Pullara, M. Leone, Aggregation kinetics of bovine serum albumin studied by FTIR spectroscopy and light scattering, Biophys. Chem. 107 (2004) 175–187.
[13] D. Carter, J.X. Ho, Serum albumin, Adv. Protein Chem. 45 (1994) 153–203.
[14] T. Kosa, T. Maruyama, M. Otagiri, Species differences of serum albumins: I. Drug binding sites, Pharm. Res. 14 (1997) 1607–1612.
[15] R.N.M. Weijers, Amino acid sequence in bovine serum albumin, Clin. Chem. 23 (1977) 1361–1362.
[16] Structure Explore-1AO6, Protein Data Bank, Department of Chemistry, Brookhaven National Laboratory, Upton, NY 11973 (http://www.pdb.bnl.gov/index.html).
[17] B.J. Berne, R. Pecora, Dynamic light scattering with application to chemistry, biology and physics, Wiley, New York, 1976.
[18] H.Z. Cummins, Light beating spectroscopy, in photon correlation and light beating spectroscopy, H. Z. Cummins and E. R. Pike Plenum, New York, 1974.
[19] P.N. Segre`, O.P. Behrend, P.N. Pusey, Short time Brownian motion in colloidal suspensions: experimental and simulation, Phys. Rev. E 52 (1995) 5070–5083.
[20] W. Brown, T. Nicolai, Dynamic light scattering, The Method and Some Application, W. Brown, Clarendon, Oxford, 1993.
[21] G.L. Ellman, Tissue sulfhydryl groups, Arch. Biochem. Biophys. 82 (1959) 70–77.
[22] H. Fabian, W. Mantele, Infrared spectroscopy of proteins, Handbook of Vibrational Spectroscopy, vol. 5, John Wiley and Sons, Chichester, 2002, p. 3999.
[23] H.H. Mantsch, D. Chapman, Infrared Spectroscopy of Biomolecules, Wiley-Liss, New York, 1996.
[24] H.A. Havel, Spectroscopic Methods for Determining Protein Structure in Solution, John Wiley and Sons, Chichester, 1995.
[25] J.H.M. Stokkum, H.L. Linsdell, J.M. Hadden, P.I. Haris, D. Chapman, M. Bloemendal, Temperature-induced changes in protein structures studied by Fourier transform infrared spectroscopy and global analysis, Biochemistry 34 (1995) 10508–10518.
[26] K. Murayama, M. Tomida, Heat-induced secondary structure and conformation change of bovine serum albumin investigated by Fourier Transform Infrared Spectroscopy, Biochemistry 43 (2004) 11526–11532.
[27] H. Fabian, C. Schultz, D. Naumann, O. Landt, U. Hahn, W.J. Saenger, Secondary structure and temperature-induced unfolding and refolding of Ribonuclease T1 in aqueous solution, Mol. Biol. 232 (1993) 967–981.
[28] Y.N. Chirgadze, O.V. Fedorov, N.P. Trushina, Estimation of amino acid residue side-chain absorption in the infrared spectra of protein solutions in heavy water, Biopolymers 14 (1975) 679–694.
[29] T. Lefevre, M. Subirade, Molecular differences in the formation and structure of fine-stranded and particulate α-lactglobulin gels, Biopolymers 54 (2000) 578–586.
[30] Ismail, H.H. Mantch, P.T.T. Wong, Aggregation of chymotrypsinogen: portrait by infrared spectroscopy, Biochim. Biophys. Acta 1121 (1992) 183–188.
[31] E.L. Gelamo, M. Tabak, Spectroscopic studies on the interaction of bovine (BSA) and human (HSA) serum albumins with ionic surfactants, Spectrochim. Acta 56 (2000) 2255–2271.
[32] L. Bagatolli, S.C. Kivatinitz, F. Aguilar, M.A. Soto, P. Sotomayor, G.D. Fidelio, Two distinguishable fluorescent modes of 1-anilino-8- napthalenesulfonate bound to human albumin, J. Floresc. 6 (1996) 33–40.
[33] P.B. Kandagal, S. Ashoka, J. Seetharamappa, S.M.T. Shaikh, Y. Jadegoud, O.B. Ijare, Study of the interaction of an anticancer drug with human and bovine serum albumin: spectroscopic approach, J. Pharm. Biomed. Anal. 41 (2006) 393–399.
[34] U. Kragh-Hansen, Molecular aspects of ligand binding to serum albumin, Pharmacol. Rev. 33 (1981) 17–53.